ACS APPLIED MATERIALS & INTERFACES

Research Article

Cite This: ACS Appl. Mater. Interfaces 2019, 11, 6009−6014

www.acsami.org

One-Step, Catalyst-Free, Scalable in Situ Synthesis of Single-Crystal Aluminum Nanowires in Confined Graphene Space

Yanan Chen,[†,∥] Yanbin Wang,[†,∥] Shuze Zhu,[‡] Chaoji Chen,[†] Valencia A. Danner,[†] Yiju Li,[†] Jiaqi Dai,[†] Hongbian Li,[†] Kun Kevin Fu,[†] Teng Li,[‡] Yang Liu,[§] and Liangbing Hu*[,†]

[†]Department of Materials Science and Engineering and [‡]Department of Mechanical Engineering, University of Maryland College Park, College Park, Maryland 20742, United States

[§]Department of Materials Science and Engineering, North Carolina State University, Raleigh, North Carolina 27606, United States

Supporting Information

ABSTRACT: Nanowires have a wide range of applications, such as transparent electrodes, Li-ion battery anodes, light-emitting diodes, solar cells, and electronic devices. Currently, aluminum (Al) nanowires can be synthesized by thermally induced substitution of germanium (Ge) nanowires, chemical vapor deposition on other metal substrates, and template-assisted growth methods. However, there are still challenges in fabricating extremely high-purity nanowires, large-scale manufacturing, and simplifying the synthesis process and conditions. Here, we report for the first time that single-crystal Al nanowires can be one-step, in situ synthesized on a reduced graphene oxide (RGO) substrate on a large scale without using any catalysts. Through a simple high temperature treatment process, commercial micro-sized Al powders in RGO film were transformed into a single-crystal Al nanowire with an average length of 1.2 μm and an average diameter of 18 nm. The possible formation mechanism of the single-crystal Al nanowires is proposed as follows: hot aluminum atoms eject from the pristine aluminum/alumina core/shell structure of Al powders when they build up enough energy from the thermal stress under high temperature and confined space conditions, which is supported by both experimental and computational results. The method introduced here can be extended to allow the synthesis of one-dimensional highly reactive materials, like alkali metal nanowires, in confined spaces.

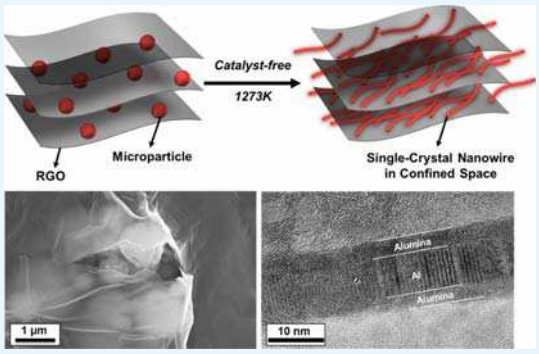

KEYWORDS: *Al nanowire, high temperature, catalyst-free, graphene, nanomanufacturing*

INTRODUCTION

Aluminum (Al) nanowires have a wide range of potential applications, such as transparent electrodes,[1,2] Al−air batteries,[3,4] Al-ion batteries,[5−7] Li-ion batteries,[8−12] transistors,[13,14] transient energy devices,[15−17] and energetic devices. Compared with the most widely used nanowires, such as Ag and Si nanowires,[17−21] Al nanowires are highly electronically conductive, extremely low in cost, and resistant to harsh environments due to the naturally compacted oxide layer on the surface. To the best of our knowledge, thermally induced substitution of germanium (Ge) nanowires, chemical vapor deposition (CVD), and template-assisted methods are the main approaches to produce high-quality Al nanowires at present.[22−25] An individual Al nanowire synthesized by the CVD method with a reaction temperature range of 125−300 °C is typically with a diameter in the range of 20−120 nm, and its straight length rarely exceeds 300 nm. Besides, Al nanowires can only grow on a substrate made of catalyst materials, such as copper and gold.[22] However, the abovementioned methods for synthesizing Al nanowires are not suitable for scalable manufacturing because of the high cost for these processes and the need of environmentally unfriendly chemicals as catalysts in these processes, which impedes the widespread applications of Al nanowires. Moreover, metallic nanowires synthesized on reduced graphene oxide (RGO) automatically form a conductive composite with an extremely high conductivity.[26,27] Such an architecture matches the need of designing advanced electronic devices,[28] but it is challenging for current scalable synthesis methods as carbon is not a typical catalyst material. Therefore, a facile and scalable synthesis strategy for Al nanowires and advanced structures is highly desired to broaden the applications of Al nanowires.

Here, we demonstrate for the first time that a one-step, catalyst-free, scalable in situ synthesis of single-crystal Al nanowires is achievable in confined graphene spaces. Before synthesizing, commercial micro-sized Al powders and graphene oxides (GO) are assembled as a laminated matrix with the assistance of vacuum filtration. After the water drains out of the

Received: November 1, 2018
Accepted: January 15, 2019
Published: January 15, 2019

DOI: 10.1021/acsami.8b18977
ACS Appl. Mater. Interfaces 2019, 11, 6009−6014

film, the micro-size Al powders are imbedded in the confined spaces created by the GO matrix. The matrix is then transferred to a furnace and is annealed at 1273 K for 1 h. The powders transform from zero-dimensional particles into one-dimensional nanowires with a uniform size distribution. Meanwhile, the GO matrix is reduced to the RGO matrix, as shown in schematic Figure 1. The proposed formation

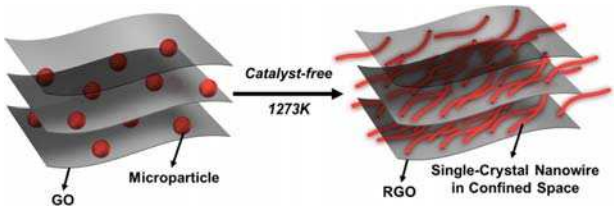

Figure 1. Schematic of catalyst-free, in situ nanowires self-assembly process. Left: Micro-sized Al powders are wrapped in between GO flakes. Right: Micro-sized Al powders are self-assembled into Al nanowires with two heads attached to the nearest RGO layers, through a one-step, catalyst-free, in situ synthesis process at a high temperature of 1273 K and in a confined space.

mechanism is that the Al powders squirt hot Al atoms when the thermal stress, caused by the thermal strain between the aluminum core and alumina shell because of different thermal expansion coefficients, accumulates to a level high enough to crack the pristine alumina shell structure of Al powders and push the aluminum atoms out. The nanowires keep growing until the atoms hit and attach to the surface of the opposite RGO sheet. The dense oxidation shell of pristine Al powders plays a critical role during the Al nanowire synthesis process, which keeps the constrain of the core part at any temperature lower than 1273 K until the Al atoms can obtain enough kinetic energy from the thermal stress. The confined space created by the laminated GO/RGO matrix is critical to stabilize the Al nanowires, which prevents the growth from interruption by gas flow, due to the impermeability of RGO to any gas including H_2 and He. In addition, the confined environment helps the formation of straight nanowires and reduces the defect density, which is extremely meaningful to exert the potential of single-crystal Al nanowires in their application on electronics. The experimental results for Al nanowire synthesis can be repeated without a precise condition control, which is essential to the scalable production and commercial manufacturing. The single-crystal Al nanowires embedded in a highly conductive matrix have great potential in various applications, such as batteries, catalysts, and transparent electrodes.

RESULTS AND DISCUSSION

To characterize the dimensional evolution, scanning electron microscopy (SEM) was conducted. The images and size distribution histograms are shown in Figure 2. An aqueous Al–GO solution is prepared under sonication for 2 h with an Al powder concentration of 2.5 mg/mL and an Al to GO weight ratio of 1:1. The dispersed GO flakes enlarge the total solid–liquid contact area and help the uniform dispersion of micro-

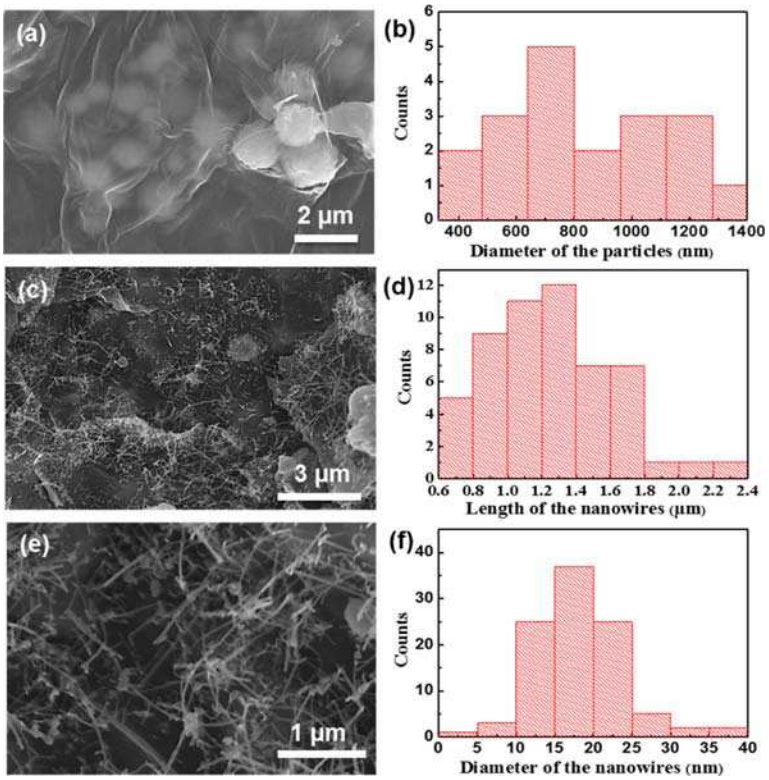

Figure 2. Transformation during the Al nanowires growth process (a) SEM image of Al powders embedded in GO film before thermal treatment with (b) an average diameter of 700 nm. (c) Al nanowires grown in the RGO film after keeping the sample at 1273 K for 1 h in argon protection with (d) an average length of 1.2 μm and (e) close-up of the RGO film with Al nanowires attached in between and (f) an average diameter of 18 nm.

DOI: 10.1021/acsami.8b18977
ACS Appl. Mater. Interfaces 2019, 11, 6009–6014

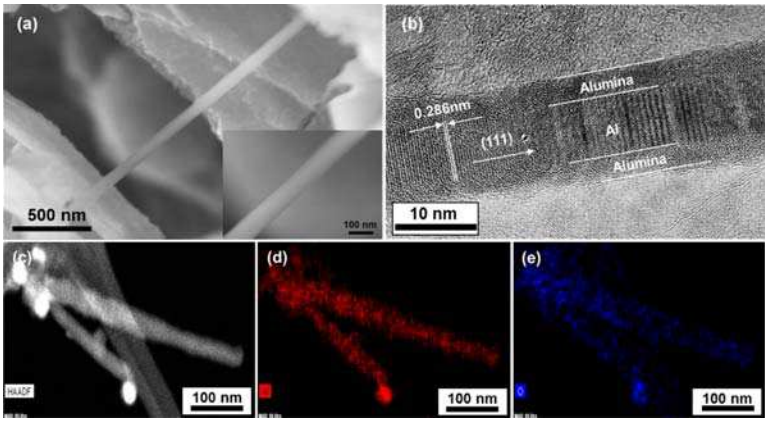

Figure 3. Characterization of Al nanowires formed in the RGO network. (a) SEM of a single Al nanowire linking two RGO layers. (b) HRTEM image of a single Al nanowire, presenting a clear single-crystal structure surrounded by a layer of amorphous alumina with a typical thickness of ~2 nm. (c–e) TEM image and the corresponding EDS mapping of Al nanowires, indicating the aluminum/alumina core/shell structure.

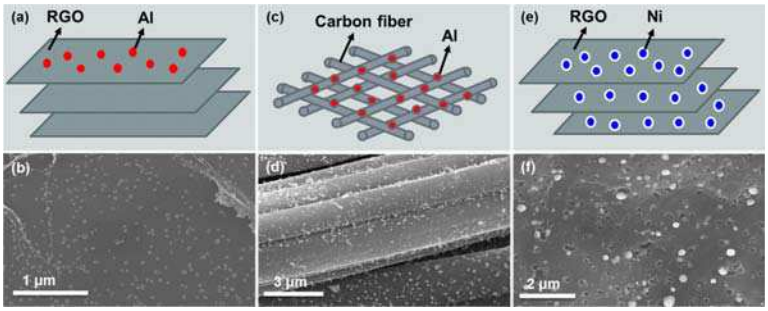

Figure 4. Formation and variation of Al nanowires under different conditions. (a,b) Schematic and experimental result illustrate that Al nanoparticles instead of Al nanowires are found on the RGO surface after high temperature treatment at 1273 K for 1 h. (c,d) Schematic and experimental result show that only trace number of Al nanowires are found on the carbon cloth surface after high temperature treatment at 1273 K for 1 h. (e,f) Schematic and SEM image show that the embedded Ni powders etch the RGO film instead of transforming to Ni nanowires after high temperature treatment at 1273 K for 1 h.

sized Al powders, allowing the Al powders to attach on the GO surface. An Al–GO thin film is made from the prepared solution by vacuum filtration. The suction force not only subtracts the water from the solution but also helps the self-assembling of GO flakes.[29] Furthermore, the interlayer distance of the complex layered structure is tunable,[30] which makes the composite more flexible to different applications. Viewed from the top view of the film surface, the pristine commercial Al powders that are held tightly by the GO matrix have a typical spherical morphology with an average diameter of 700 nm (Figure 2a,b). The spherical Al powders disappeared after 1 h high temperature annealing at 1273 K in an argon atmosphere, and the RGO film is filled by nanowires with an average length of 1.2 μm in a range of 0.6–2.4 μm (Figure 2c,d), which is about four times longer than that reported using the CVD method.[22] We found that 1273 K was almost the lowest temperature where a large number of Al nanowires formed, and Al powders converted into ultrafine nanoparticles after much higher temperature treatment as we reported in recent work.[31−36] The long and straight nanowires in Figure 2c indicate that not much stress accumulates during the nanowire formation process. The Al nanowires synthesized by our method have a high growing rate and the surface stress tends to decrease rather than increase when the Al powders transfer from zero dimension to one dimension. On the contrary, for the Al nanowires grown by CVD,[22] with a slow growing rate, the strain accumulates during the formation process thus their straight segment rarely exceeds 300 nm. The nanowires have an average diameter of 18 nm in a range of 1–40 nm filling the gap between two neighbor RGO flakes (Figure 2e,f). More SEM images for Al nanowires are shown in Figure S1 (Supporting Information). In addition, the atomic force microscopy (AFM) image confirms the morphology of the Al nanowire (Figure S2a–c, Supporting Information), which is consistent with the above statistical results. The single Al nanowire in the AFM image is prepared by dropping the Al nanowire ink onto glass, and experimental details are shown in Supporting Information

To characterize and evaluate the morphology and the chemical component of the nanowires, high resolution transmission electron microscopy (HRTEM) and energy dispersive spectroscopy (EDS) were carried out. The SEM image shows a randomly picked single Al nanowire grown in between the RGO layers (Figure 3a). Its straight segment length is beyond 1 μm, and no bending or folding is observed. The HRTEM image of an Al nanowire shows that a crystalline structure grows along (111) with a lattice distance of 0.286 nm, presenting a clear single-crystal structure surrounded by a layer of amorphous alumina with a typical thickness of ~2 nm (Figure 3b).[37] There is no twining boundary found throughout the nanowires, which indicates not much strain built during the growth. According to previous computational work, twinning

DOI: 10.1021/acsami.8b18977
ACS Appl. Mater. Interfaces 2019, 11, 6009–6014

only appears when the Al crystal deforms at a high strain rate.[38,39] This observation provides the evidence and support to our purposed formation mechanism that strain is released at the beginning of the synthesis. More TEM images for single-crystal Al nanowires are shown in Figure S3 (Supporting Information). The TEM image and the corresponding EDS mapping of Al nanowires in Figure 3c−e exhibit the core/shell structure with an aluminum core and an aluminum oxidation shell, confirming the amorphous alumina layer in Figure 3b. The chemical composition of a single Al nanowire detected by EDS displays an Al−O ratio of about 2.2:1 in atoms (Figure S4, Supporting Information). The oxygen atoms mainly come from two sources: the oxygen released during the reduction of GO, and the alumina shell of the Al powders. Besides aluminum, carbon, and oxygen; no other elements are observed from EDS studies.

To investigate the synthesis conditions and underlying mechanism for Al nanowires, a series of control experiments were conducted. It is worthy to note that no nanowire can be found after receiving the same high temperature treatment process when the pristine Al powders were only distributed on the surface of a RGO film, as shown in the schematic and SEM image (Figure 4a,b). The result indicates that the confined space created by RGO flakes can prevent the growth from interruption by gas flow, due to the impermeability of RGO to any gas including H_2 and He.[40] When the substrate was changed to a carbon cloth, that is, a porous carbon base, the Al powders cannot be fully blocked away from the influence of the gas flow under a high-temperature treatment. As expected, only a few nanowires were observed, confirming that the confined space greatly affects the yield of nanowires (Figure 4c,d). To fully understand the role that the oxidation layers (alumina layer) of the pristine Al powders play, we switched the embedded material to nickel powders that do not naturally have a dense oxidized layer due to the reason that nickel metal is not as easily oxidized as aluminium. The schematic and SEM image (Figure 4e,f) show that Ni powders etched the RGO film instead of forming any one-dimensional structure under the same high temperature treatment condition.

The formation mechanism of the catalyst-free synthesized Al nanowires in a confined space is proposed, as presented in schematic Figure 5a. A tensile stress accumulates inside the aluminium oxide shell with increasing temperature because of the difference of thermal expansion coefficients of Al and Al_2O_3. The particle squirts hot Al atoms when the stress is high enough to crack the oxidation layer. We propose that Al nanowires grow toward the free space confined by graphene flakes driven by the temperature gradients and pressure gradients, and amorphous Al_2O_3 continuously diffuses to the nanowire surface. The Al_2O_3 shell terminates the growth in the lateral direction so as to induce the growth of nanowires in the one-dimensional direction. Single-crystal Al nanowires are formed and stabilized in the confined space after the sample cools down. To shed light on the mechanism of the hot Al atoms squirting out at such a high temperature, we have conducted molecular dynamics simulations to validate our hypothesis. We have constructed a model in which an Al nanoparticle with a radius of 2.3 nm is pressured by an artificial sphere whose radius is 2.5 nm (see Supporting Information for simulation details).[41,42] We use the large-scale atomic/molecular massively parallel simulator (LAMMPS) to perform molecular dynamics simulations. The nonbonded interaction between artificial points in the sphere and the Al atoms in the

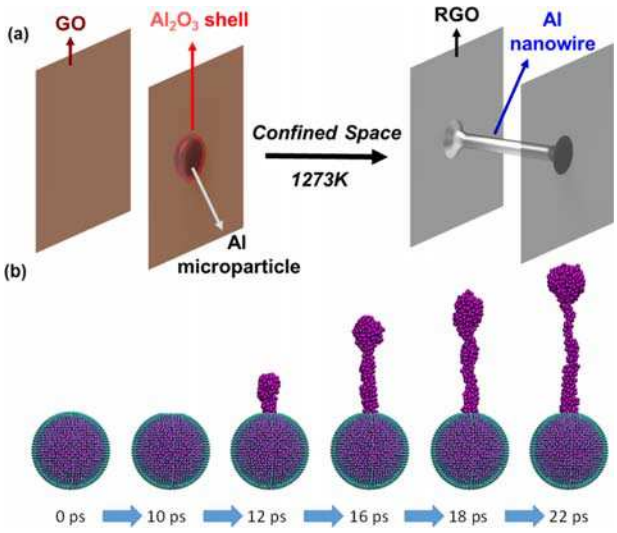

Figure 5. Formation mechanism of Al nanowires (a) schematic shows the formation of nanowires. The fracture of the aluminum oxide shell allows the enclosed Al atoms to form nanowires. (b) Molecular dynamics simulation illustrates the formation process. Sudden fracture of the aluminum oxide shell is modeled by suddenly removing a shallow spherical cap of the shell after 10 ps. With the temperature of 1300 K, the Al nanoparticle begins to squirt Al atoms through the vent. An increasing number of Al atoms come out from the vent and thus initiate the formation of nanowires. Such squiring is not observed at the temperature of 300 K.

nanoparticle is modeled by the Lennard-Jones 12-6 potential, while the embedded atom (EAM) potential file with the LAMMPS distribution to describe the bonded interaction between Al atoms in the nanoparticle. We model the sudden fracture of the aluminum oxide shell by suddenly removing a shallow spherical cap after 10 ps, and thereby forming a vent. The simulation is performed on a canonical ensemble, controlled by a Nosé−Hoover thermostat. For the case of 1300 K, the Al nanoparticle begins to squirt Al atoms through the vent on the artificial sphere. At 22 ps, an increasing number of Al atoms come out from the vent and reach as high as 10 nm above the vent (Figure 5b). Such squirting is caused by the high pressure in the Al nanoparticle built up from the increased temperature. For a control simulation, we have also investigated the dynamics of the Al nanoparticle at 300 K. In this case, the built-up pressure is not able to induce a significant squirting behavior (see Supporting Information for simulation details).

CONCLUSIONS

For the first time, we report single-crystal Al nanowires with an average length of 1.2 μm and average diameter of 18 nm, can be in situ synthesized inside a conductive RGO matrix driven by high-temperature treatment. The synthesis process of Al nanowires is simple (one-step), scalable, and cost-efficient using commercially available Al powders as the starting material, which shows great commercial potential. Moreover, this in situ methodology for Al nanowire production does not need any catalyst, exhibiting promising potential toward environmentally friendly manufacturing. The possible formation mechanism of Al nanowires, supported by molecular dynamics simulations, is proposed that the Al powders squirt hot Al atoms when the thermal stress, caused by the thermal

DOI: 10.1021/acsami.8b18977
ACS Appl. Mater. Interfaces 2019, 11, 6009−6014

strain between the aluminum core and the alumina shell due to different thermal expansion coefficients, accumulates to a level high enough to crack the pristine alumina shell structure of Al powders. This method for synthesizing nanowires can be potentially applicable to a wide range of materials by designing the pristine core/shell structure, which calls for further investigation. The as-synthesized single-crystal Al nanowires embedded in a highly conductive matrix can be widely used for energetic materials, Li-ion/Al-ion batteries, catalysts, transparent electrodes, flexible devices, and many other emerging applications.

EXPERIMENTAL SECTION

Synthesis of Al Nanowires. Commercial micro-sized Al powders (99.5%, Sigma-Aldrich) in ethanol (4 mg/mL) were mixed with GO solution (2 mg/mL) by shaking and sonication to form a uniform Al−GO suspension. The GO was synthesized by an improved Hummer's method. A freestanding Al−GO film was obtained by filtering the Al−GO solution through a 0.65 μm pore-sized membrane (Millipore, USA) followed by drying in air for 12 h in order to detach the film from the membrane. The as-obtained film containing precursors was then transferred to a tube furnace under argon atmosphere and was held at 1273 K for 1 h.

Material Characterization. The morphology of the Al nanowire was investigated by a Hitachi SU-70 field emission scanning electron microscope (FE-SEM), JEOL JEM 2100 transmission electron microscope at an accelerating voltage of 200 kV, and Veeco NanoScope-III MultiMode AFM.

Molecular Dynamics Simulations. We use the LAMMPS to perform molecular dynamics simulations. The nonbonded interaction between artificial points in the sphere and the Al atoms in nanoparticles is modeled by the Lennard-Jones 12-6 potential $V(r) = 4\epsilon\left(\frac{\sigma^{12}}{r^6} - \frac{\sigma^6}{r^6}\right)$ with the parameters ϵ = 0.0122492 eV, σ = 0.40 nm. The parameters are the average between Al−Al and Al−O interaction parameters (ϵ_{Al-Al} = 0.0218968 eV, σ_{Al-Al} = 0.4499 nm, ϵ_{Al-O} = 0.0026016 eV, σ_{Al-O} = 0.35 nm), which are developed through the customary Lorentz−Berthelot mixing rules from the universal force field (a full periodic table force field for molecular mechanics and molecular dynamics simulations[42]). We use the EAM potential file with the LAMMPS distribution to describe the bonded interaction between Al atoms in the nanoparticle. The simulation is performed on a canonical ensemble, controlled by a Nosé−Hoover thermostat. The time step is 0.0001 ps. Two temperatures, 300 K and 1300 K, are considered. Before running dynamic simulations, the energy of the system is first minimized by using conjugate gradient algorithm until either the total energy change between successive iterations divided by the energy magnitude is less than or equal to 10^{-6} or the total force is less than 10^{-5} eV/Å. The first 100 000 timesteps (total equal to 10 ps) are performed with the artificial sphere intact. Then the aforementioned spherical cap is suddenly removed while the dynamic simulation keeps running.

ASSOCIATED CONTENT

Supporting Information

The Supporting Information is available free of charge on the ACS Publications website at DOI: 10.1021/acsami.8b18977.

Six figures showing SEM, TEM images of Al nanowires, AFM image of Al nanowires, and digital photo image of Al nanowires solution, EDS for Al nanowires and atomistic model of Al nanoparticles (PDF)

AUTHOR INFORMATION

Corresponding Author

*E-mail: binghu@umd.edu.

ORCID

Chaoji Chen: 0000-0001-9553-554X
Yiju Li: 0000-0001-9240-5686
Hongbian Li: 0000-0002-9806-3223
Liangbing Hu: 0000-0002-9456-9315

Author Contributions

‖Y.C. and Y.W.contributed equally to this work.

Notes

The authors declare no competing financial interest.

ACKNOWLEDGMENTS

This project is supported by an NSF Scalable Nanomanufacturing Grant #1635221. Dr. Hu acknowledges the financial support from the dean's office for the equipment setup. We acknowledge the support of the Maryland NanoCenter and its NispLab. Y.C. acknowledges China Scholarship Council (CSC) for financial support. T.L. and S.Z. acknowledge the University of Maryland supercomputing resources (http://hpcc.umd.edu) made available for conducting the research reported in this paper.

REFERENCES

(1) Hu, L.; Kim, H. S.; Lee, J.-Y.; Peumans, P.; Cui, Y. Scalable Coating and Properties of Transparent, Flexible, Silver Nanowire Electrodes. *ACS Nano* **2010**, *4*, 2955−2963.

(2) Hu, L.; Wu, H.; Cui, Y. Metal Nanogrids, Nanowires, and Nanofibers for Transparent Electrodes. *MRS Bull.* **2011**, *36*, 760−765.

(3) Zhang, X.; Yang, S. H.; Knickle, H. Novel Operation and Control of an Electric Vehicle Aluminum/air Battery System. *J. Power Sources* **2004**, *128*, 331−342.

(4) Cho, Y.-J.; Park, I.-J.; Lee, H.-J.; Kim, J.-G. Aluminum anode for aluminum-air battery - Part I: Influence of aluminum purity. *J. Power Sources* **2015**, *277*, 370−378.

(5) Wang, W.; Jiang, B.; Xiong, W.; Sun, H.; Lin, Z.; Hu, L.; Tu, J.; Hou, J.; Zhu, H.; Jiao, S. A New Cathode Material for Super-Valent Battery Based on Aluminium Ion Intercalation and Deintercalation. *Sci. Rep.* **2013**, *3*, 3383.

(6) Sun, H.; Wang, W.; Yu, Z.; Yuan, Y.; Wang, S.; Jiao, S. A New Aluminium-Ion Battery with High Voltage, High Safety and Low Cost. *Chem. Commun.* **2015**, *51*, 11892−11895.

(7) Lin, M.-C.; Gong, M.; Lu, B.; Wu, Y.; Wang, D.-Y.; Guan, M.; Angell, M.; Chen, C.; Yang, J.; Hwang, B.-J.; Dai, H. An Ultrafast Rechargeable Aluminium-Ion Battery. *Nature* **2015**, *520*, 324−328.

(8) Kuksenko, S. P. Aluminum Foil as Anode Material of Lithium-Ion Batteries: Effect of Electrolyte Compositions on Cycling Parameters. *Russ. J. Electrochem.* **2013**, *49*, 67−75.

(9) Li, S.; Niu, J.; Zhao, Y. C.; So, K. P.; Wang, C.; Wang, C. A.; Li, J. High-Rate Aluminium Yolk-Shell Nanoparticle Anode for Li-Ion Battery with Long Cycle Life and Ultrahigh Capacity. *Nat. Commun.* **2015**, *6*, 7872.

(10) Li, Q.; Bjerrum, N. J. Aluminum as Anode for Energy Storage and Conversion: A Review. *J. Power Sources* **2002**, *110*, 1−10.

(11) Chan, C. K.; Peng, H.; Liu, G.; McIlwrath, K.; Zhang, X. F.; Huggins, R. A.; Cui, Y. High-Performance Lithium Battery Anodes Using Silicon Nanowires. *Nat. Nanotechnol.* **2007**, *3*, 31−35.

(12) Yang, Y.; Jeong, S.; Hu, L.; Wu, H.; Lee, S. W.; Cui, Y. Transparent Lithium-Ion Batteries. *Proc. Natl. Acad. Sci. U.S.A.* **2011**, *108*, 13013−13018.

(13) Ju, S.; Facchetti, A.; Xuan, Y.; Liu, J.; Ishikawa, F.; Ye, P.; Zhou, C.; Marks, T. J.; Janes, D. B. Fabrication of Fully Transparent Nanowire Transistors for Transparent and Flexible Electronics. *Nat. Nanotechnol.* **2007**, *2*, 378−384.

(14) Ju, S.; Li, J.; Liu, J.; Chen, P.-C.; Ha, Y.-g.; Ishikawa, F.; Chang, H.; Zhou, C.; Facchetti, A.; Janes, D. B.; Marks, T. J. Transparent Active Matrix Organic Light-Emitting Diode Displays Driven by Nanowire Transistor Circuitry. *Nano Lett.* **2008**, *8*, 997−1004.

DOI: 10.1021/acsami.8b18977
ACS Appl. Mater. Interfaces 2019, 11, 6009−6014

(15) Fu, K. K.; Wang, Z.; Dai, J.; Carter, M.; Hu, L. Transient Electronics: Materials and Devices. *Chem. Mater.* **2016**, *28*, 3527−3539.
(16) Fu, K. K.; Wang, Z.; Yan, C.; Liu, Z.; Yao, Y.; Dai, J.; Hitz, E.; Wang, Y.; Luo, W.; Chen, Y.; Kim, M.; Hu, L. All-Component Transient Lithium-Ion Batteries. *Adv. Energy Mater.* **2016**, *6*, 1502496.
(17) Cui, L.-F.; Ruffo, R.; Chan, C. K.; Peng, H.; Cui, Y. Crystalline-Amorphous Core−Shell Silicon Nanowires for High Capacity and High Current Battery Electrodes. *Nano Lett.* **2009**, *9*, 491−495.
(18) Lee, J.-Y.; Connor, S. T.; Cui, Y.; Peumans, P. Solution-Processed Metal Nanowire Mesh Transparent Electrodes. *Nano Lett.* **2008**, *8*, 689−692.
(19) Wu, H.; Kong, D.; Ruan, Z.; Hsu, P.-C.; Wang, S.; Yu, Z.; Carney, T. J.; Hu, L.; Fan, S.; Cui, Y. A Transparent Electrode Based on a Metal Nanotrough Network. *Nat. Nanotechnol.* **2013**, *8*, 421−425.
(20) Wu, H.; Hu, L.; Rowell, M. W.; Kong, D.; Cha, J. J.; McDonough, J. R.; Zhu, J.; Yang, Y.; McGehee, M. D.; Cui, Y. Electrospun Metal Nanofiber Webs as High-Performance Transparent Electrode. *Nano Lett.* **2010**, *10*, 4242−4248.
(21) Cui, Y.; Lieber, C. M. Functional Nanoscale Electronic Devices Assembled Using Silicon Nanowire Building Blocks. *Science* **2001**, *291*, 851−853.
(22) Benson, J.; Boukhalfa, S.; Magasinski, A.; Kvit, A.; Yushin, G. Chemical Vapor Deposition of Aluminum Nanowires on Metal Substrates for Electrical Energy Storage Applications. *ACS Nano* **2011**, *6*, 118−125.
(23) Hashoosh, A.; Hirshy, H.; Brousseau, E. B.; Moosa, A. Fabrication of Aluminium Nanowires by Differential Pressure Injection. *ISRN Nanomater.* **2013**, *2013*, 1.
(24) Huber, C. A.; Huber, T. E.; Sadoqi, M.; Lubin, J. A.; Manalis, S.; Prater, C. B. Nanowire Array Composites. *Science* **1994**, *263*, 800−802.
(25) Singh, M.; Wang, J.; Tian, M.; Zhang, Q.; Pereira, A.; Kumar, N.; Mallouk, T. E.; Chan, M. H. W. Synthesis and Superconductivity of Electrochemically Grown Single-Crystal Aluminum Nanowires. *Chem. Mater.* **2009**, *21*, 5557−5559.
(26) Balandin, A. A. Thermal Properties of Graphene and Nanostructured Carbon Materials. *Nat. Mater.* **2011**, *10*, 569−581.
(27) Fang, R. R.; He, Y. Z.; Zhang, K.; Li, H. Melting Behavior of Aluminum Nanowires in Carbon Nanotubes. *J. Phys. Chem. C* **2014**, *118*, 7622−7629.
(28) Javey, A.; Nam; Friedman, R. S.; Yan, H.; Lieber, C. M. Layer-by-Layer Assembly of Nanowires for Three-Dimensional, Multifunctional Electronics. *Nano Lett.* **2007**, *7*, 773−777.
(29) Liu, G.; Jin, W.; Xu, N. Graphene-Based Membranes. *Chem. Soc. Rev.* **2015**, *44*, 5016−5030.
(30) Cheng, C.; Jiang, G.; Garvey, C. J.; Wang, Y.; Simon, G. P.; Liu, J. Z.; Li, D. Ion Transport in Complex Layered Graphene-Based Membranes with Tuneable Interlayer Spacing. *Sci. Adv.* **2016**, *2*, No. e1501272.
(31) Li, T.; Pickel, A. D.; Yao, Y.; Chen, Y.; Zeng, Y.; Lacey, S. D.; Li, Y.; Wang, Y.; Dai, J.; Wang, Y.; Yang, B.; Fuhrer, M. S.; Marconnet, A.; Dames, C.; Drew, D. H.; Hu, L. Thermoelectric properties and performance of flexible reduced graphene oxide films up to 3,000 K. *Nat. Energy* **2018**, *3*, 148−156.
(32) Yao, Y.; Huang, Z.; Xie, P.; Lacey, S. D.; Jacob, R. J.; Xie, H.; Chen, F.; Nie, A.; Pu, T.; Rehwoldt, M.; Yu, D.; Zachariah, M. R.; Wang, C.; Shahbazian-Yassar, R.; Li, J.; Hu, L. Carbothermal shock synthesis of high-entropy-alloy nanoparticles. *Science* **2018**, *359*, 1489−1494.
(33) Chen, Y.; Xu, S.; Li, Y.; Jacob, R. J.; Kuang, Y.; Liu, B.; Wang, Y.; Pastel, G.; Salamanca-Riba, L. G.; Zachariah, M. R.; Hu, L. FeS_2 Nanoparticles Embedded in Reduced Graphene Oxide toward Robust, High-Performance Electrocatalysts. *Adv. Energy Mater.* **2017**, *7*, 1700482.
(34) Li, Y.; Chen, Y.; Nie, A.; Lu, A.; Jacob, R. J.; Gao, T.; Song, J.; Dai, J.; Wan, J.; Pastel, G.; Zachariah, M. R.; Yassar, R. S.; Hu, L. In Situ, Fast, High-Temperature Synthesis of Nickel Nanoparticles in Reduced Graphene Oxide Matrix. *Adv. Energy Mater.* **2017**, *7*, 1601783.
(35) Chen, Y.; Li, Y.; Wang, Y.; Fu, K.; Danner, V. A.; Dai, J.; Lacey, S. D.; Yao, Y.; Hu, L. Rapid, in Situ Synthesis of High Capacity Battery Anodes through High Temperature Radiation-Based Thermal Shock. *Nano Lett.* **2016**, *16*, 5553−5558.
(36) Chen, Y.; Egan, G. C.; Wan, J.; Zhu, S.; Jacob, R. J.; Zhou, W.; Dai, J.; Wang, Y.; Danner, V. A.; Yao, Y.; Fu, K.; Wang, Y.; Bao, W.; Li, T.; Zachariah, M. R.; Hu, L. Ultra-Fast Self-Assembly and Stabilization of Reactive Nanoparticles in Reduced Graphene Oxide Films. *Nat. Commun.* **2016**, *7*, 12332.
(37) McClain, M. J.; Schlather, A. E.; Ringe, E.; King, N. S.; Liu, L.; Manjavacas, A.; Knight, M. W.; Kumar, I.; Whitmire, K. H.; Everitt, H. O.; Nordlander, P.; Halas, N. J. Aluminum Nanocrystals. *Nano Lett.* **2015**, *15*, 2751−2755.
(38) Warner, D. H.; Curtin, W. A.; Qu, S. Rate Dependence of Crack-Tip Processes Predicts Twinning Trends in F.c.c. Metals. *Nat. Mater.* **2007**, *6*, 876−881.
(39) Chen, M.; Ma, E.; Hemker, K. J.; Sheng, H.; Wang, Y.; Cheng, X. Deformation Twinning in Nanocrystalline Aluminum. *Science* **2003**, *300*, 1275−1277.
(40) Su, Y.; Kravets, V. G.; Wong, S. L.; Waters, J.; Geim, A. K.; Nair, R. R. Impermeable Barrier Films and Protective Coatings Based on Reduced Graphene Oxide. *Nat. Commun.* **2014**, *5*, 4843.
(41) Plimpton, S. Fast Parallel Algorithms for Short-Range Molecular Dynamics. *J. Comput. Phys.* **1995**, *117*, 1−19.
(42) Rappe, A. K.; Casewit, C. J.; Colwell, K. S.; Goddard, W. A.; Skiff, W. M. UFF, a Full Periodic Table Force Field for Molecular Mechanics and Molecular Dynamics Simulations. *J. Am. Chem. Soc.* **1992**, *114*, 10024−10035.

DOI: 10.1021/acsami.8b18977
ACS Appl. Mater. Interfaces 2019, 11, 6009−6014